Diagn Interv Radiol 2025; DOI: 10.4274/dir.2024.242800

ABDOMINAL IMAGING

ORIGINAL ARTICLE

Computed tomography-based contrast features for distinguishing extra-gastrointestinal stromal tumors from intra-abdominal fibromatosis

Lijing Zhang[1]
Yongbo Li[1]
Xinxin Luo[1]
Deqi Li[1]
Linlin Yin[2]
Jiayue Li[3]
Li Zhang[1]

[1]Cangzhou Central Hospital, Department of Radiology, Cangzhou, China

[2]Cangzhou Central Hospital, Department of Laboratory, Cangzhou, China

[3]Cangzhou Renmin Hospital, Department of Radiology, Cangzhou, China

PURPOSE

This study aims to define the computed tomography (CT) criteria that distinguish extra-gastrointestinal stromal tumors (eGISTs) from intra-abdominal fibromatosis (IAF).

METHODS

Retrospective analysis was conducted on CT images obtained from 31 pathologically confirmed cases, including 17 cases of eGISTs and 14 of IAF. Various parameters [e.g., lesion location, contour characteristics, border delineation, enhancement patterns, presence of intralesional necrosis, vessels, air, fat, and hemorrhage, the long diameter (LD), LD/short diameter (SD) ratio, and volume (LD × SD × height diameter)] were meticulously evaluated. In addition, the degree of enhancement during arterial and portal venous phases and the lesion-to-aorta CT attenuation ratio during both phases were quantified. Statistical analysis was performed using Fisher's exact test, the Student's t-test, and the receiver operating characteristic curve to identify significant CT criteria. Sensitivity and specificity assessments were conducted for single and combined CT criteria.

RESULTS

Significant differentiators between eGISTs and IAF include non-mesenteric localization, irregular contour, well-defined borders, heterogeneous enhancement, presence of intralesional necrosis and vessels, and absence of intralesional fat, with LD exceeding 9.6 cm, an LD/SD ratio >1.22, and volume surpassing 603.3 cm^3 ($P < 0.05$). A combination of seven or more of these criteria yielded a specificity of 100%.

CONCLUSION

Ten distinct CT criteria have been identified to distinguish eGISTs from IAF, notably encompassing non-mesenteric localization, irregular contour, well-defined borders, heterogeneous enhancement, presence of intralesional necrosis and vessels, absence of intralesional fat, LD >9.6 cm, an LD/SD ratio >1.22, and volume surpassing 603.3 cm^3.

CLINICAL SIGNIFICANCE

The current findings establish CT criteria to distinguish eGISTs from IAF in a clinical setting.

KEYWORDS

Diagnosis, computed tomography criteria, non-mesenteric localization, intralesional necrosis, heterogeneous enhancement

Corresponding author: Li Zhang

E-mail: 18031792007@163.com

Received 17 April 2024; revision requested 02 May 2024; last revision received 13 May 2024; accepted 09 June 2024.

Epub: 22 July 2024

Publication date: 30.12.2024

DOI: 10.4274/dir.2024.242800

Extra-gastrointestinal stromal tumors (eGISTs) are a rare type of gastrointestinal stromal tumor (GIST). They occur outside the gastrointestinal tract and are not associated with the intestinal wall.[1] Approximately 80% (26/32) of eGISTs are intra-abdominal, primarily in the mesentery and omentum, with some detected in the retroperitoneum.[2] A pioneering report in 1999, documenting 26 cases originating from the omentum and mesentery, highlighted their clinicopathological and immunohistochemical similarities to GISTs, leading to their classification as eGISTs.[3] Most reported eGISTs present as large lesions (>10 cm) or exhibit high mitotic activity (>10/50 high-power field), placing them in a high-risk category with an unfavorable prognosis.[2,4,5] Diagnosis typically involves preoperative identification using

You may cite this article as: Zhang L, Li Y, Luo X, et al. Computed tomography-based contrast features for distinguishing extra-gastrointestinal stromal tumors from intra-abdominal fibromatosis. *Diagn Interv Radiol.* 2025;31(1):10-16.

radiological imaging modalities such as contrast-enhanced computed tomography (CT) or magnetic resonance imaging, followed by confirmation through postoperative histopathological and immunohistochemical analyses. Histologically, eGISTs are characterized by spindle, epithelioid, and/or pleomorphic cell morphology and are associated with positive immunostaining for CD117 (c-kit receptor) and CD34 biomarkers.[5]

A subtype of aggressive fibromatosis (AF), intra-abdominal fibromatosis (IAF) has the lowest incidence rate, representing a rare benign monoclonal fibroblastic proliferation that primarily originates from the mesentery or retroperitoneum within the abdomen.[6] Despite its benign classification, IAF is notable for its high recurrence rate post-surgical resection, with no propensity for metastasis.[7] Although IAF and eGISTs are distinct entities, they are prone to misidentification.[7-10] As a widely employed non-invasive medical imaging modality, CT plays a pivotal role in examining abdominal structures to detect lesions.[7] Consequently, differentiating between eGISTs and IAF on CT images is crucial because of their distinct prognoses and treatment modalities. However, accurate diagnosis remains challenging for personalized treatment and prognosis evaluation given the rarity of both intra-abdominal eGISTs and IAF.

Considering the scarcity of literature clarifying the distinctive CT features and clinical attributes of both eGISTs and IAF, we conducted a retrospective analysis of clinical data and CT images from 31 patients observed at a single center. Among these patients, 17 were diagnosed with intra-abdominal eGISTs and 14 with IAF. We aimed to provide a comprehensive synthesis of their clinical profiles and CT characteristics, thereby enhancing our understanding of their inherent behaviors. By identifying unique features on contrast-enhanced CT scans, we sought to mitigate the risk of inappropriate or subpar treatment strategies.

Main points

- The computed tomography (CT) images of patients with extra-gastrointestinal stromal tumors (eGISTs) and intra-abdominal fibromatosis (IAF) have crucial differences.
- The 10 discerning CT criteria to distinguish eGISTs from IAF are non-mesenteric localization, irregular contour, well-defined borders, heterogeneous enhancement, presence of intralesional necrosis and vessels, absence of intralesional fat, long diameter (LD) >9.6 cm, an LD/ short diameter ratio >1.22, and volume exceeding 603.3 cm^3.
- These 10 CT criteria can be utilized in clinical practice to distinguish eGISTs from IAF before surgery.

Methods

Patient characteristics

This retrospective study received approval from the Institutional Review Board at Cangzhou Central Hospital (decision no: #2021-266-02, date: 09.05.2021), which waived the requirement for informed consent. We screened 224 patients with GISTs who underwent surgical procedures at our hospital between July 2013 and December 2021. Among them, 19 cases were confirmed as eGISTs (Figure 1). Additionally, all 15 cases of IAF included in our institutional database were compiled from routine clinical practice during the same period. The inclusion criteria were as follows: surgical excision of the tumor, complete clinicopathological data, and preoperative contrast-enhanced CT scans of good image quality. The exclusion criteria were irresectable tumors (one case caused by multiple focal lesions for eGISTs and one case caused by liver metastasis) or the absence of preoperative contrast-enhanced CT scans (one case with only plain CT for IAF). Ultimately, 31 patients (17 with intra-abdominal eGISTs and 14 with IAF) were included in this study. Clinical data, including age, sex, presence of abdominal mass, and abdominal pain, were carefully reviewed.

Computed tomography image acquisition

All 31 patients underwent comprehensive abdominal and/or pelvic contrast-enhanced CT examinations covering the entire tumor, using a 320-detector row scanner (Toshiba Medical Systems, Otawara, Japan) at our institution. The CT imaging parameters were standardized as follows: tube voltage was set at 120 kV, tube current ranged from 100 to 450 mA, rotation time was 0.5 s, detector collimation was set at 64 × 0.625 mm, matrix size was 512 × 512, pitch ratio was 0.6–1.2:1, and slice thickness was 5 mm. For dynamic contrast-enhanced CT imaging, an intravenous non-ionic contrast agent (1 mL/kg) was administered using an automatic power injector at a rate of 3.5 mL/s. Images of the arterial and portal venous phases were acquired at 25–30 and 60 s post-injection, respectively. It is important to note that delayed-phase imaging was omitted in this retrospective study due to its absence in routine abdominal CT protocols. The reconstruction of CT images from both phases was performed with a slice thickness of 2 mm. Additionally, coronal and sagittal multiplanar reformatted (MPR) images were generated to ascertain the lesions' origin relative to the gastrointestinal tract wall.

Image analysis

The contrast-enhanced CT images were independently reviewed by two seasoned abdominal radiologists (with 11 and 9 years of experience, respectively), following a randomized sequence using a picture archiving and communication system. Both readers conducted evaluations without any knowledge of the clinical findings or pathological results. Qualitative analysis of the CT criteria included evaluating lesion location, contours, borders, enhancement pattern, and the presence of intralesional necrosis, vessels, air, fat, and hemorrhage. Lesion locations were validated using MPR CT images and surgical records and were stratified as either mesenteric or non-mesenteric regions. Lesion contours were categorized as round, ovoid, lobulated, or irregular, with round and ovoid shapes classified as regular and lobulated and irregular shapes as irregular. Lesion

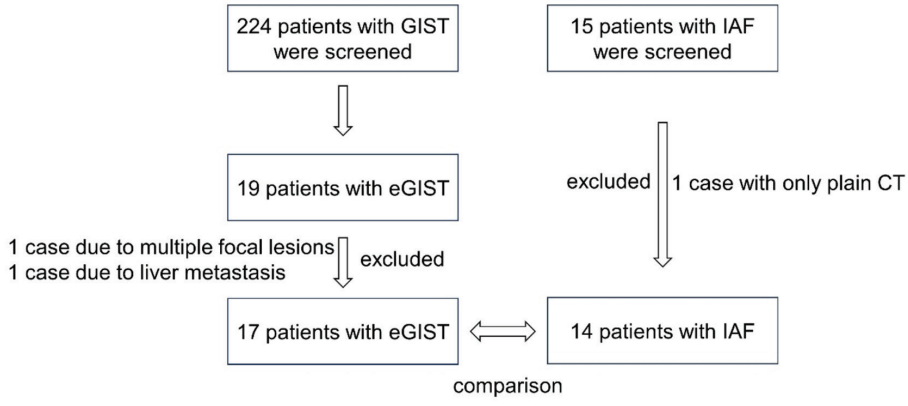

Figure 1. Study flowchart. GIST, gastrointestinal stromal tumor; eGIST, extra-gastrointestinal stromal tumors; CT, computed tomography; IAF, intra-abdominal fibromatosis.

borders were delineated as ill-defined or well-defined in relation to the adjacent soft tissue. Enhancement patterns, characterized as homogeneous or heterogeneous, were assessed during the portal venous phase. Homogeneous enhancement was identified by a difference of <10 HU between the most strongly and weakly enhanced regions, whereas >10 HU signified heterogeneous enhancement. Intralesional low attenuation, suggesting necrosis, was designated by a CT attenuation value of <20 HU on the portal venous phase. Intralesional vessel identification was based on feeding vessels observed in MPR images during the arterial phase. Intralesional low attenuation, indicating gas, was identified by a CT attenuation value similar to the gas density in the stomach or intestine during the arterial–venous phase. Similarly, intralesional low attenuation, suggesting fat, was delineated by a CT attenuation value similar to subcutaneous fat during the arterial–venous phase. Intralesional hyperattenuation, indicating hemorrhage, was recognized by a CT attenuation value of >70 HU, persisting across both arterial and portal venous phases. In cases of disagreement, the radiologists engaged in a discussion to achieve consensus. The quantitative analysis included assessing the long diameter (LD), LD/short diameter (SD) ratio, volume [LD × SD × height diameter (HD)], degree of enhancement (DE) during both arterial and portal venous phases, and lesion/aorta (L/A) CT attenuation ratio. Consensus was reached by averaging measurements from the two readers to determine the final result for qualitative data analysis.

Statistical analysis

All statistical analyses were conducted using the SPSS statistical package (version 26.0, SPSS, Chicago, IL, USA). The required sample size was determined using PS software (version 3.0.12). A *P* value of <0.05 was considered statistically significant. Fisher's exact test was used to compare qualitative data between the eGIST and IAF groups, and the Student's t-test was utilized for comparing quantitative data. After statistical analysis, sensitivity and specificity values were calculated for each CT criterion that showed a significant difference between eGISTs and IAF. Sensitivity and specificity values were computed for the LD, LD/SD ratio, and volume (LD × SD × HD) to generate receiver operating characteristic (ROC) curves. These curves helped determine the optimal cut-off points for distinguishing IAF from eGISTs. The optimal cut-off point was identified as the value that maximized the sum of sensitivity and specificity.

Results

Clinical characteristics

This study involved a cohort of 31 patients, 17 individuals diagnosed with intra-abdominal eGISTs and 14 with IAF, to outline distinctive clinical characteristics and CT features observed on contrast-enhanced CT images. The cohort consisted of 10 men and 7 women in the eGISTs group, with a mean age of 60.94 ± 2.90 years, and 6 men and 8 women in the IAF group, with a mean age of 54.29 ± 4.03 years. The clinical characteristics of the patients with are summarized in Table 1. The analysis revealed no significant differences in age, sex, or the presence of abdominal pain and abdominal mass between the two tumor types (all $P > 0.05$).

Qualitative analysis of computed tomography features

The qualitative analysis of CT features comparing eGISTs and IAF is summarized in Table 2. The distribution of tumor location differed significantly between the two tumor types ($P = 0.021$). Furthermore, eGISTs were more commonly found in the non-mesenteric region, whereas IAF occurred more frequently in the mesenteric region. In terms of lesion contour, most eGISTs exhibited a lobulated or irregular shape, whereas most IAF cases presented with an ovoid or round contour ($P = 0.001$). Moreover, eGISTs tended to have well-defined borders, whereas most IAF lesions demonstrated ill-defined borders ($P = 0.001$). The enhancement pattern significantly differentiated between eGISTs and IAF ($P < 0.001$), with heterogeneous enhancement observed more frequently in eGISTs. In addition, eGISTs exhibited a higher tendency toward intralesional necrosis compared with IAF ($P < 0.001$), whereas IAF lesions showed less frequent intralesional necrosis. Regarding intralesional vessels, eGISTs displayed a higher tendency, whereas IAF had less frequent intralesional vessels ($P < 0.001$). By contrast, IAF demonstrated a greater tendency toward intralesional fat, whereas eGISTs had less frequent intralesional fat ($P = 0.004$). However, intralesional hemorrhage and intralesional air did not significantly differentiate between eGISTs and IAF. Representative images illustrating these qualitative CT features are presented in Figures 2a-c. These findings emphasize the utility of qualitative CT analysis in distinguishing between eGISTs and IAF, providing valuable insights for accurate diagnosis and treatment planning.

Quantitative analysis of computed tomography features

Table 2 provides a summary of the quantitative analysis of CT features comparing eGISTs and IAF. eGISTs exhibited a larger LD and volume compared with IAF ($P < 0.001$) and displayed a higher LD/SD ratio than IAF ($P = 0.003$). However, the DE during the arterial phase and venous phase and the L/A ratio (arterial phase, portal venous phase) did not reveal significant differences between eGISTs and IAF in this study. Representative images are presented in Figure 2a-c.

Based on the ROC analysis results, the LD had a cut-off value of 9.6 cm for the differential diagnosis of eGISTs and IAF, achieving a sensitivity of 82.4%, a specificity of 82.9%, and an area under the ROC curve of 0.912. Similarly, the volume had a cut-off value that resulted in 94.1% sensitivity, 85.7% specificity, and an area under the ROC curve of 0.903. Additionally, the LD/SD ratio had a cut-off value that led to 82.4% sensitivity, 71.4% specificity, and an area under the ROC curve of 0.826. The LD exhibited similar performance compared with volume and LD/SD ratio (DeLong test, $P < 0.05$); the ROC curves are displayed in Figure 3.

Table 1. Clinical characteristics analysis results for eGISTs versus IAF

Clinical characteristics		eGISTs (n = 17)	IAF (n = 14)	*P* value
Age (mean ± SD)		60.94 ± 2.90	54.29 ± 4.03	0.181[b]
Sex	Man	10 (58.8%)	6 (42.9%)	0.479[a]
	Woman	7 (41.2%)	8 (57.1%)	
Abdominal mass	Present	8 (47.1%)	6 (42.9%)	1.000[a]
	Absent	9 (52.1%)	8 (57.1%)	
Abdominal pain	Present	7 (41.2%)	11 (78.6%)	0.067[a]
	Absent	10 (58.8%)	3 (21.4%)	

$P < 0.05$ indicates that the difference is statistically significant. [a]: Between eGISTs and IAF compared with Fisher's exact test. [b]: Between eGISTs and IAF compared with the Student's t-test. SD, standard deviation; eGISTs, extra-gastrointestinal stromal tumors; IAF, intra-abdominal fibromatosis.

Sensitivity and specificity values for computed tomography diagnosis

Table 3 displays the sensitivity and specificity values of each significant CT criterion for distinguishing eGISTs from IAF. The combination of any 5 of these 10 criteria resulted in a sensitivity of 100% (17 of 17) and a specificity of 92.9% (13 of 14). When employing any seven or more of these criteria, a specificity of 100% was achieved, as indicated in Table 4.

Discussion

eGISTs constitute a rare subset of malignant mesenchymal tumors that share clinicopathological and immunohistochemical features with GISTs.[3] Although reports suggest eGISTs can appear in various anatomical sites such as the neck,[11] liver,[12,13] and prostate,[14] the abdomen remains the predominant location,[15] often involving the mesentery, omentum, and retroperitoneum.[16] It is widely acknowledged that eGISTs demonstrate aggressive behavior and have an unfavorable prognosis.[2,5,15] Despite being distinct entities, eGISTs and IAF are frequently confused.[7-10] The differentiation between these entities carries significant clinical implications, as the diagnostic criteria for malignancy in eGISTs do not apply to IAF. Unlike eGISTs, which are prone to metastasis and exhibit aggressive behavior, IAF represents benign tumors with no metastatic potential, although they can be locally aggressive. Therefore, clarifying the distinction between eGISTs and IAF is crucial for appropriate treatment planning and prognostic assessment.

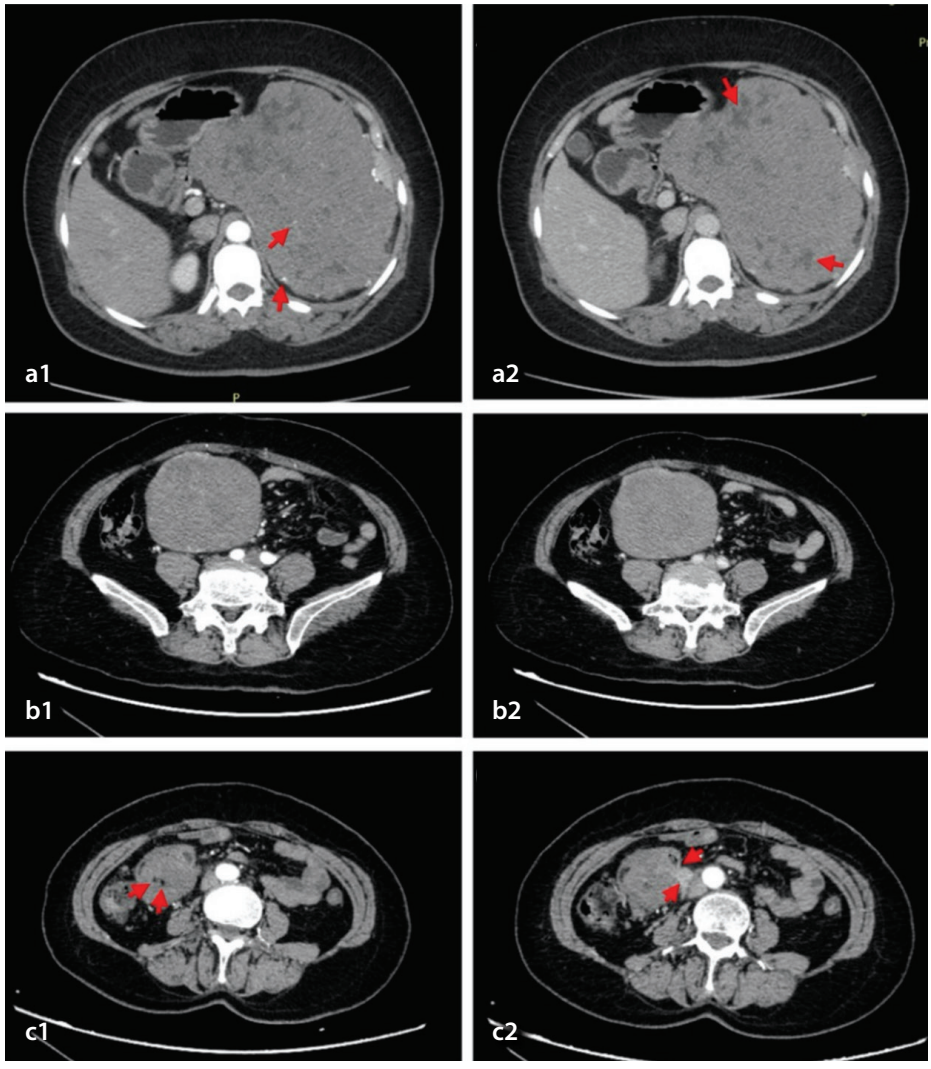

Figure 2. (a) A 50-year-old woman with a 17.1-cm-long diameter extra-gastrointestinal stromal tumor in the space between the stomach and spleen. **(a1)** Axial arterial phase computed tomography (CT) image revealing an irregular mass with a well-defined border and intralesional vessels (arrows). **(a2)** Portal venous phase axial contrast-enhanced CT images revealing a heterogeneously enhanced mass with intralesional necrosis (arrows). **(b)** A 57-year-old woman with a 9.4-cm-long diameter intra-abdominal fibromatosis (IAF) arising from transverse colon mesentery. **(b1)** Axial arterial phase CT image revealing a regular mass with a well-defined border without intralesional vessels. **(b2)** Portal venous phase axial contrast-enhanced CT images revealing a homogeneously enhanced mass without intralesional necrosis. **(c)** A 53-year-old woman with a 5.3-cm-long diameter IAF arising from duodenal mesentery. **(c1)** Axial arterial phase CT image revealing punctate intralesional fat (arrows). **(c2)** Axial arterial phase CT image displaying an involved descending duodenal segment (arrow).

For both eGISTs and IAF, abdominal pain and a palpable mass are the most common clinical symptoms.[6,17] In this study, we observed no significant differences in the presence of abdominal pain, abdominal mass, age, or sex between the tumor types ($P > 0.05$). However, we encountered two intriguing cases of IAF where a palpable mass was distinctly observed in the initial plain CT scan, subsequently shifting to another location within the abdomen in the contrast-enhanced CT scan. This observation suggests that the mass exhibited mobility along the mesentery, originating from the mesenteric region.

Our study identified 10 CT criteria as statistically significant indicators for distinguishing between eGISTs and IAF: non-mesenteric location, irregular contour, well-defined border, heterogeneous enhancement, presence of intralesional necrosis and vessels, absence of intralesional fat, LD >9.6 cm, volume >603.3 cm^3, and an LD/SD ratio >1.22. Moreover, combining positive CT criteria improved the diagnostic performance for distinguishing eGISTs from IAF, thereby facilitating accurate diagnosis and appropriate treatment selection.

In our study, eGISTs exhibited a significantly larger LD and volume compared with IAF ($P < 0.001$), as well as a higher LD/SD ratio than IAF ($P = 0.003$). These findings are consistent with previous literature, which suggests that patients with eGISTs often remain asymptomatic until the lesion progresses to a palpable mass.[18] Given the demands of our routine workflow and heavy reporting load, measuring the LD in axial CT images proves to be a practical and cost-effective approach. Our analysis identified a 9.6-cm cut-off value for the LD in axial images as an effective discriminator between eGISTs and IAF, yielding a sensitivity of 82.4%, a specificity of 82.9%, and an area under the ROC curve of 0.912. Notably, this performance was comparable with that of volume and LD/SD ratio ($P > 0.05$ for the DeLong test). In contrast to previous reports that encompassed all GIST cases, our study focused specifically on eGISTs because of their fundamental differences from GISTs.[16] Interestingly, in our analysis, both DE (arterial and venous phases) and L/A ra-

tio (arterial and portal venous phases) for eGISTs and IAF did not exhibit significant differences, diverging from previous findings. We observed that eGISTs tended to have a larger average volume (1,840.68 cm^3) compared with IAF (459.74 cm^3), potentially resulting in the dispersion of intra-tumor vessels and subsequent reduction in CT attenuation values. However, significant factors for distinguishing eGISTs from IAF included the enhancement pattern and the presence of intralesional necrosis and vessels. Our results indicated that eGISTs predominantly exhibited heterogeneous enhancement (94.1% of cases), intralesional necrosis (94.1% of cases), and intralesional vessels (94.1% of cases) on contrast CT. These findings align with previous reports, underscoring the characteristic features of eGISTs, including heterogeneous contrast enhancement, prominent intralesional vessels, and inner low attenuation changes attributed to necrosis, hemorrhage, or cystic degeneration, which contrast with the CT features observed in IAF in our study.

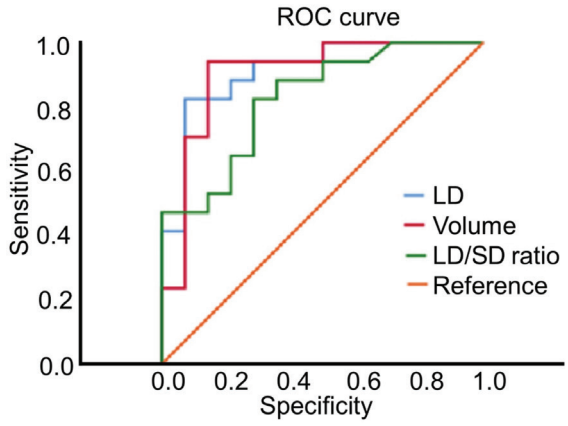

Figure 3. Receiver operating characteristic (ROC) curve. Graph displaying four ROC curves for long diameter (LD), volume, and LD/short diameter (SD) ratio to differentiate eGISTs from IAF. The areas under the ROC curve are 0.816 (LD), 0.861 (volume), and 0.888 (LD/SD ratio). eGISTs, extra-gastrointestinal stromal tumors, IAF, intra-abdominal fibromatosis.

Table 2. Qualitative and quantitative CT image analyses results for eGISTs versus IAF

CT criteria		eGISTs (n = 17)	IAF (n = 14)	*P* value
Location	Mesenteric region	9 (52.9%)	13 (92.9%)	0.021[a]
	Non-mesenteric region	8 (47.1%)	1 (7.1%)	
Contour	Regular	5 (29.4%)	13 (92.9%)	0.001[a]
	Irregular	12 (70.6%)	1 (7.1%)	
Border	Well-defined	17 (100%)	7 (50%)	0.001[a]
	Ill-defined	0 (0%)	7 (50%)	
Enhancement pattern	Homogeneous	1 (5.9%)	12 (85.7%)	<0.001[a]
	Heterogeneous	16 (94.1%)	2 (14.3%)	
Intralesional necrosis	Present	16 (94.1%)	0 (0%)	<0.001[a]
	Absent	1 (5.9%)	14 (100%)	
Intralesional vessels	Present	16	4	<0.001[a]
	Absent	1	10	
Intralesional air	Present	2 (11.8%)	2 (14.3%)	1.000[a]
	Absent	15 (88.2%)	12 (85.7%)	
Intralesional fat	Present	0 (0%)	6 (42.9%)	0.004[a]
	Absent	17 (100%)	8 (57.1%)	
Intralesional hemorrhage	Present	2 (11.8%)	0 (0%)	0.488[a]
	Absent	15 (88.2%)	14 (100%)	
LD		13.50 ± 1.01	6.74 ± 0.82	<0.001[b]
LD/SD ratio		1.56 ± 0.11	1.17 ± 0.03	0.003[b]
Volume (LD × SD × HD)		1840.68 ± 264.46	459.74 ± 196.43	<0.001[b]
DE (AP, HU)		49.10 ± 3.24	48.37 ± 2.19	0.860[b]
DE (PP, HU)		65.67 ± 4.46	61.77 ± 2.65	0.482[b]
L/A ratio (AP)		0.17 ± 0.01	0.17 ± 0.01	0.856[b]
L/A ratio (PP)		0.46 ± 0.02	0.45 ± 0.03	0.780[b]

Data are presented as means ± standard deviations. [a]: Between eGISTs and IAF compared with Fisher's exact test. [b]: Between eGISTs and IAF compared with the Student's t-test. CT, computed tomography; eGISTs, extra-gastrointestinal stromal tumors; IAF, intra-abdominal fibromatosis; LD, long diameter; SD, short diameter; HD, height diameter; DE, degree of enhancement; L/A ratio, lesion/aorta CT attenuation ratio; AP, arterial phase; PP, portal venous phase.

In this study, IAF was more frequently located in the mesenteric region (92.9%, 13/14) compared with eGISTs (52.9%, 9/17), a finding consistent with prior research.[6] Intra-abdominal AF, a rare and locally aggressive mass, originates from benign fibrous tissue proliferation[7] and represents the most common primary tumor of the mesentery.[19] In our series, 70.6% (12/17) of eGIST cases exhibited lobulated or irregular contours, whereas 92.9% (13/14) of IAF cases demonstrated ovoid or round shapes, deviating from typical pathological descriptions of eGISTs.[17] Intra-abdominal AF is characterized by a highly collagenous stroma, often homogenous and with soft-tissue attenuation.[20] In our study, 50% (7/14) of IAF cases displayed ill-defined margins on contrast CT, indicative of its locally aggressive growth pattern, a distinct CT feature from eGISTs. We propose that the ill-defined mass represents an aggressive phenotype for IAF, necessitating pathological confirmation in future studies. Another distinguishing CT feature is the presence of intralesional fat, observed in 42.9% (6/14) of IAF cases compared with 0% (0/17) of eGIST cases, which is consistent with previous findings.[9] As IAF gradually enlarges, it infiltrates mesenteric fat, signaling a locally aggressive growth pattern distinct from eGISTs. This unique growth pattern underscores the differential diagnosis between IAF and eGISTs and highlights the importance of considering both clinical and radiological features in making an accurate diagnosis.

The treatment approach for both eGISTs and IAF involves multidisciplinary team management, which is paramount for optimizing patient outcomes.[7] The standard treatment

Table 3. PPV, NPV, sensitivity, and specificity values of each significant CT criteria for differentiating eGISTs from IAF

CT criteria	PPV	NPV	Sensitivity (%)	Specificity (%)
Non-mesenteric region	88.9 (8/9)	59.1 (13/22)	47.1 (8/17)	92.9 (13/14)
Irregular contour	92.3 (12/13)	72.2 (13/18)	70.6 (12/17)	92.9 (13/14)
Well-defined border	70.8 (17/24)	100 (7/7)	100 (17/17)	50 (7/14)
Heterogeneous enhancement	88.9 (16/18)	92.3 (12/13)	94.1 (16/17)	85.7 (12/14)
Intralesional necrosis presence	100 (16/16)	93.3 (14/15)	94.1 (16/17)	100 (14/14)
Intralesional vessels presence	80 (16/20)	90.9 (10/11)	94.1 (16/17)	71.4 (10/14)
Intralesional fat absence	68 (17/25)	100 (6/6)	100 (17/17)	42.9 (6/14)
LD >9.6 cm	93.3 (14/15)	81.3 (13/16)	82.4 (14/17)	92.9 (13/14)
Volume >603.3 cm^3	88.9 (16/18)	92.3 (12/13)	94.1 (16/17)	85.7 (12/14)
LD/SD ratio >1.22	77.8 (14/18)	76.9 (10/13)	82.4 (14/17)	71.4 (10/14)

PPV, positive predictive value; NPV, negative predictive value; CT, computed tomography; eGISTs, extra-gastrointestinal stromal tumors; IAF, intra-abdominal fibromatosis; LD, long diameter; SD, short diameter.

Table 4. Combined CT criteria in differentiating eGISTs from IAF

CT criteria	eGISTs (n = 17)	IAF (n = 14)	Sensitivity (%)	Specificity (%)
≥1	17	12	100	14.3
≥2	17	9	100	35.7
≥3	17	4	100	71.4
≥4	17	2	100	85.7
≥5	17	1	100	92.9
≥6	16	1	94.1	92.9
≥7	16	0	94.1	100
≥8	15	0	88.2	100
≥9	14	0	82.3	100
≥10	10	0	58.8	100

CT, computed tomography; eGISTs, extra-gastrointestinal stromal tumors; IAF, intra-abdominal fibromatosis.

for GIST involves radical surgical resection, often combined with adjuvant imatinib therapy for cases classified as medium or high risk according to National Institutes of Health criteria.[21] Unfortunately, eGISTs have an unfavorable prognosis despite treatment strategies mirroring those of GISTs. Common treatment modalities for managing IAF include surgery alone or in combination with radiotherapy.[6] In certain cases, a multidisciplinary approach encompassing surgery, chemotherapy, and radiation therapy is advocated.[22]

Several limitations were encountered in our study. First, due to the low incidence rates of both eGISTs and IAF, our sample size was limited. Future research with larger sample sizes is warranted to provide a more comprehensive understanding of the biological behavior of both tumor entities. Second, immunohistochemical markers are crucial in delineating the distinct characteristics of eGISTs and IAF. Further investigation and correlation studies between these two tumors are warranted. Third, the routine abdominal CT protocols utilized in our study did not include delayed phase imaging to minimize unnecessary radiation exposure.

In conclusion, this study identifies effective CT criteria to differentiate eGISTs from IAF. A total of 10 main parameters were determined, and the 3 CT parameters with the highest diagnostic accuracy were LD >9.6 cm, heterogeneous enhancement, and well-defined borders.

Conflict of interest disclosure

The authors declared no conflicts of interest.

References

1. Ambrosio M, Testa AC, Moro F, et al. Imaging in gynecological disease (19): clinical and ultrasound features of extragastrointestinal stromal tumors (eGIST). *Ultrasound Obstet Gynecol*. 2020;56(5):749-758. [Crossref]
2. Reith JD, Goldblum JR, Lyles RH, Weiss SW. Extragastrointestinal (soft tissue) stromal tumors: an analysis of 48 cases with emphasis on histologic predictors of outcome. *Mod Pathol*. 2000;13(5):577-585. [CrossRef]
3. Miettinen M, Monihan JM, Sarlomo-Rikala M, et al. Gastrointestinal stromal tumors/smooth muscle tumors (GISTs) primary in the omentum and mesentery: clinicopathologic and immunohistochemical study of 26 cases. *Am J Surg Pathol*. 1999;23(9):1109-1118. [CrossRef]
4. Acar T, Efe D, Okuş A, Öcal İ, Harman M. A rare solid tumor of the retroperitoneum with venous extension and lung metastasis: extra-gastrointestinal stromal tumor. *Turk J Gastroenterol*. 2015;26(4):358-359. [CrossRef]
5. Hu W, Zheng C, Li R, et al. Retroperitoneal extragastrointestinal stromal tumors have a poor survival outcome: a multicenter observational study. *Cancer Manag Res*. 2020;12(10):10491-10504. [CrossRef]
6. Xiao J, Mao J, Li B. Clinical characteristics and treatment of intra-abdominal aggressive fibromatosis: a retrospective study of 16 patients. *Front Med (Lausanne)*. 2020;7(1):2. [CrossRef]
7. Zhu H, Chen H, Zhang S, Peng W. Intra-abdominal fibromatosis: differentiation from gastrointestinal stromal tumour based on biphasic contrast-enhanced CT findings. *Clin Radiol*. 2013;68(11):1133-1139. [CrossRef]
8. Kim JH, Ryu MH, Park YS, Kim HJ, Park H, Kang YK. Intra-abdominal desmoid tumors mimicking gastrointestinal stromal tumors - 8 cases: a case report. *World J Gastroenterol*. 2019;25(16):2010-2018. [CrossRef]
9. Yantiss RK, Spiro IJ, Compton CC, Rosenberg AE. Gastrointestinal stromal tumor versus intra-abdominal fibromatosis of the bowel wall: a clinically important differential diagnosis. *Am J Surg Pathol*. 2000;24(7):947-957. [CrossRef]
10. Rodriguez JA, Guarda LA, Rosai J. Mesenteric fibromatosis with involvement of the gastrointestinal tract. A GIST simulator: a study of 25 cases. *Am J Clin Pathol*. 2004;121(1):93-98. [CrossRef]
11. Zhang Y, Zhang A, Song L, Li X, Zhang W. Primary extragastrointestinal stromal tumor

on FDG PET/CT. *Clin Nucl Med*. 2018;43(9):705-706. [CrossRef]

12. Joyon N, Dumortier J, Aline-Fardin A, et al. Gastrointestinal stromal tumors (GIST) presenting in the liver: diagnostic, prognostic and therapeutic issues. *Clin Res Hepatol Gastroenterol*. 2018;42(2):23-28. [CrossRef]
13. Qian XH, Yan YC, Gao BQ, Wang WL. Prevalence, diagnosis, and treatment of primary hepatic gastrointestinal stromal tumors. *World J Gastroenterol*. 2020;26(40):6195-6206. [CrossRef]
14. Li L, Hu ZQ, Yang CG, et al. Current knowledge of primary prostatic extra-gastrointestinal stromal tumor: a case report and review of the literature. *J Int Med Res*. 2021;49(5):3000605211013172. [CrossRef]
15. Uzunoglu H, Tosun Y. Primary extra gastrointestinal stromal tumors of the abdomen. *North Clin Istanb*. 2021;8(5):464-471. [CrossRef]
16. Yi JH, Park BB, Kang JH, et al. Retrospective analysis of extra-gastrointestinal stromal tumors. *World J Gastroenterol*. 2015;21(6):1845-1850. [CrossRef]
17. Zhu J, Yang Z, Tang G, Wang Z. Extragastrointestinal stromal tumors: computed tomography and magnetic resonance imaging findings. *Oncol Lett*. 2015;9(1):201-208. [CrossRef]
18. Iqbal N, Sharma A, Iqbal N. Clinicopathological and treatment analysis of 13 extragastrointestinal stromal tumors of mesentery and retroperitoneum. *Ann Gastroenterol*. 2015;28(1):105-108. [CrossRef]
19. Levy AD, Rimola J, Mehrotra AK, Sobin LH. From the archives of the AFIP: benign fibrous tumors and tumorlike lesions of the mesentery: radiologic-pathologic correlation. *Radiographics*. 2006;26(1):245-264. [CrossRef]
20. Einstein DM, Tagliabue JR, Desai RK. Abdominal desmoids: CT findings in 25 patients. *AJR Am J Roentgenol*. 1991;157(2):275-279. [CrossRef]
21. Gold JS, Gönen M, Gutiérrez A, et al. Development and validation of a prognostic nomogram for recurrence-free survival after complete surgical resection of localised primary gastrointestinal stromal tumour: a retrospective analysis. *Lancet Oncol*. 2009;10(11):1045-1052. [CrossRef]
22. Rampone B, Pedrazzani C, Marrelli D, Pinto E, Roviello F. Updates on abdominal desmoid tumors. *World J Gastroenterol*. 2007;13(45):5985-5988. [CrossRef]